Int. J. Heat Mass Transfer. Vol. 11, pp. 943–962. Pergamon Press 1968. Printed in Great Britain

TURBULENT HEAT TRANSFER IN A TUBE WITH PRESCRIBED HEAT FLUX

SHU HASEGAWA† and YASUNOBU FUJITA‡
Department of Nuclear Engineering, Kyushu University, Fukuoka, Japan

(*Received* 10 *September* 1967)

Abstract—An approximate method is proposed to predict Nusselt number for turbulent flow in a tube with an arbitrary axially varying heat flux distribution. Evaluation of sums of infinite series with poor convergency is required for this method and done correctly. The predicted results by the proposed method were examined experimentally with air for uniform heat flux, exponentially varying heat flux and rectilinearly varying heat flux. The experimental apparatus was so constructed that heat flux could distribute in the prescribed manner by changing axially the cross sectional area of the tube wall conducted low voltage a.c. Predicted Nusselt numbers are in good agreement with the experimental data.

The conditions for heat flux distributions which have the fully developed situation with generalized temperature profile invariant in the axial direction were analysed theoretically. As the result, it is found the exponentially varying heat flux alone can realize the fully developed situation. Both cases of uniform heat flux and uniform wall temperature, which have been well known to realize the fully developed situation, correspond to the special cases of exponentially varying heat flux.

NOMENCLATURE

a, thermal diffusivity;
B_n, coefficient corresponding to eigen-value;
c_p, specific heat;
C_n, eigen-value;
d, tube inner diameter;
D, tube outer diameter;
$e(x)$, heat generation distribution per unit tube length;
$E(x)$, $\int_0^x e(x)\,dx$;
g, dimensionless total thermal diffusivity, $1 + \varepsilon_H/a$;
G, volumetric flow rate;
h, heat-transfer coefficient;
k, thermal conductivity;
K, overall heat-transfer coefficient;
Nu, Nusselt number, hd/k;
Nu_H, Nusselt number for uniform heat flux;
Nu_T, Nusselt number for uniform wall temperature;
Pr, Prandtl number, ν/a;
q, heat flux;
Q_E, total heat input;
r, radial distance;
r_0, tube inner radius, $d/2$;
Re, Reynolds number, $u_a d/\nu$;
s, dimensionless radial distance, r/r_0;
T, temperature;
T_c, temperature at tube center;
T_{in}, inlet temperature;
T_R, ambient temperature;
u, velocity in axial direction;
u_a, mean velocity in axial direction;
u^+, dimensionless velocity, $u/\sqrt{(\tau_w/\rho)}$;
v, dimensionless velocity, u/u_a;
x, axial distance;
X, dimensionless axial distance, x/d;
X_0, dimensionless axial distance with uniform heat flux;
y, distance from tube wall, $r_0 - r$;
y^+, dimensionless distance from tube wall, $y\sqrt{(\tau_w/\rho)}/\nu$;

† Professor of Nuclear Engineering, Kyushu University, Fukuoka, Japan. Member of J.S.M.E.

‡ Lecturer of Mechanical Engineering, Kyushu University. Member of J.S.M.E.

z, dimensionless axial distance, $x/2r_0RePr$;
Z, dimensionless axial distance, $X - X_0$.

Greek symbols
α, parameter related to heat flux distribution;
γ, specific weight;
ε_H, eddy diffusivity for heat;
ε_M, eddy diffusivity for momentum;
η, parameter related to coefficient of index of exponential function;
θ, dimensionless temperature, $(T_w - T)/(2r_0q/k)$;
ν, kinematic viscosity;
ρ, fluid density;
τ_w, shear stress at tube wall;
φ, dimensionless temperature, $\theta_m - \theta$.

Subscripts
fd, fully developed conditions;
m, mixed mean conditions;
w, wall conditions.

INTRODUCTION

HEAT transfer to turbulent flow in tubes and ducts has been a subject of continuing interest for many years. And most of the investigations are concerned with the fully developed situation under the two cases of the uniform heat flux and the uniform wall temperature distributions in the axial direction. On the contrary heat transfer for undeveloped or developing situation is now under study by many investigators. The problem of heat transfer for axially varying heat flux, which belongs in this category, has drawn a great deal of attention and much consideration has been paid to the sinusoidal heat flux distribution [1] in relation to the cooling of nuclear reactors. But general treatment of this problem is relatively rare in previous investigations. The present investigation is made on the general treatment which can be applicable to the heat-transfer problem of any arbitrary heat flux distribution.

Analytical treatment for arbitrary heat flux or wall temperature distribution in the axial direction is mainly based on the superposition technique because of the linear and homogeneous nature of the energy equation. The solution to be superposed is the thermal-entry-solution for the uniform heat flux or the uniform wall temperature. For flow in a tube, this solution is obtained by solving the eigen-value problem and consequently the solution takes the form of the infinite series consisting of the eigen function corresponding to each eigen value. In actual calculation higher terms of the infinite series must be neglected. If the solution can be expressed satisfactorily with fewer terms, the convergency of the series solution is said to be good or fast. The same comments also hold true for the superposed solution because it takes the form of the infinite series. The infinite series contained in the superposed solution for prescribed heat flux distribution show poor convergent nature in contrast with those for prescribed wall temperature distribution. Probably to avoid this drawback, Hall and Price [2] evaluated the theoretical solution for the exponentially varying heat flux by integrating graphically the thermal-entry-solution for uniform heat flux which was obtained experimentally and compared it with the experimental results.

In this paper analytical solution for arbitrary heat flux distribution is investigated with respect to the convergency and an approximate method is proposed to make up for the poor convergency of the solution. This method needs a few sums of the infinite series consisting of the eigenvalues and the corresponding coefficients of the thermal-entry-solution under the uniform heat flux conditions. Though it is very difficult to evaluate these sums properly for poor convergency of the infinite series, the evaluation is done conveniently. In relation to the axial variation of Nusselt number, theoretical investigation is made on what cases the fully developed situation is obtained when the prescribed axially varying heat flux is given.

As the result, only the case with the exponentially varying heat flux is found to have the fully developed situation. Experimental support of the proposed method is performed with air for several heat flux distributions.

The similar method to the proposed one is applicable to the forced convection heat-transfer problem with axially varying heat flux for flow in the ducts, the annular space and the two parallel plates, the thermal-entry-solution of which belongs to the eigen-value problem and therefore takes the form of the infinite series.

ANALYTICAL SOLUTION

A schematic diagram showing the coordinate system is given in Fig. 1.

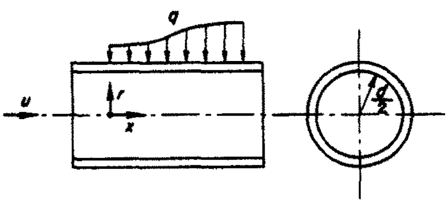

FIG. 1. Coordinate system.

For the prescribed heat flux distribution $q(x)$ in the axial direction x, the temperature difference between the wall temperature T_w and the mixed mean temperature T_m of the fluid at an axial position x is expressed as [3]

$$T_w - T_m = -\frac{2}{kRe}\sum_{n=1}^{\infty} F_n\beta_n^2 \int_0^x q(w) \times \exp\left(-\frac{4\beta_n^2}{Re} \times \frac{x-w}{2r_0}\right) dw, \quad (1)$$

where k is thermal conductivity of the fluid, Re Reynolds number, r_0 tube radius, β_n^2 and F_n are eigen-values and corresponding coefficients respectively which appear in the thermal-entry-solution of the energy equation under the uniform heat flux conditions. The first five eigen-values and corresponding coefficients have been found using Deissler's turbulent velocity profile by Siegel and Sparrow [3], numerical values of which are reproduced in Table 1, where $B_n = -F_n/2$ and $C_n = 4\beta_n^2/Re$.

Introducing the symbols B_n and C_n and the dimensionless variables $X = x/2r_0$ and $W = w/2r_0$, then the local Nusselt number at an axial position X, which has usual definition

$$Nu = \frac{hd}{k} = \frac{q}{T_w - T_m} \times \frac{d}{k},$$

where h is heat-transfer coefficient, takes the following expression with the aid of equation (1).

$$\frac{1}{Nu} = \sum_{n=1}^{\infty} B_n C_n \frac{\int_0^X q(w)\exp(C_n W)\,dW}{q(X)\exp(C_n X)}. \quad (2)$$

Now take the axial coordinates shown in Fig. 2 and suppose heat flux distribution expressed as

$$q = q_0 \qquad \text{for} \qquad X \leqslant X_0,$$

and

$$q = q_0 F(Z) = q_0\{1 + H(Z)\} \qquad \text{for} \qquad X \geqslant X_0,$$

where q_0 is a constant and $F(Z)$ and $H(Z)$ are functions of Z.

Then Nusselt number at the position Z is

$$\frac{1}{Nu} = \sum_{n=1}^{\infty} B_n \frac{1 - \exp(-C_n X_0)}{F(Z)\exp(C_n Z)} + \sum_{n=1}^{\infty} B_n C_n \frac{\int_0^Z F(W')\exp(C_n W')\,dW'}{F(Z)\exp(C_n Z)}$$

$$= \sum_{n=1}^{\infty} B_n \frac{1 - \exp\{-C_n(X_0 + Z)\}}{1 + H(Z)} + \sum_{n=1}^{\infty} B_n C_n \frac{\int_0^Z H(W')\exp(C_n W')\,dW'}{\{1 + H(Z)\}\exp(C_n Z)}. \quad (3)$$

Table 1. Listing of B_n and C_n (reproduced from reference [3])

				$Re = 50000$					
	$Pr = 0·7$			$Pr = 1·0$			$Pr = 10$		
n	B_n	C_n	B_n/C_n	B_n	C_n	B_n/C_n	B_n	C_n	B_n/C_n
1	$1·7535 \times 10^{-3}$	0·1110	$15·797 \times 10^{-3}$	$1·2525 \times 10^{-3}$	0·1104	$11·345 \times 10^{-3}$	$1·3265 \times 10^{-4}$	0·1093	$12·136 \times 10^{-4}$
2	0·9240	0·2984	3·097	0·6710	0·2964	2·264	0·7730	0·2921	2·646
3	0·6390	0·5632	1·135	0·4743	0·5585	0·849	0·6065	0·5480	1·107
4	0·4921	0·9064	0·543	0·3740	0·8976	0·417	0·5530	0·8767	0·631
5	0·4105	1·3280	0·309	0·3205	1·3128	0·244	0·5545	1·2760	0·435
$\sum_{n=1}^{5}$	$4·2191 \times 10^{-3}$	—	$20·881 \times 10^{-3}$	$3·0923 \times 10^{-3}$	·	$15·119 \times 10^{-3}$	$3·8135 \times 10^{-4}$	—	$16·955 \times 10^{-4}$
				$Re = 100000$					
	$Pr = 0·7$			$Pr = 1·0$			$Pr = 10$		
n	B_n	C_n	B_n/C_n	B_n	C_n	B_n/C_n	B_n	C_n	B_n/C_n
1	$0·9870 \times 10^{-3}$	0·1018	$9·695 \times 10^{-3}$	$0·6875 \times 10^{-3}$	0·1015	$6·773 \times 10^{-3}$	$0·7130 \times 10^{-4}$	0·1010	$7·059 \times 10^{-4}$
2	0·5170	0·2729	1·894	0·3689	0·2718	1·357	0·3986	0·2697	1·478
3	0·3555	0·5140	0·692	0·2569	0·5116	0·502	0·2944	0·5064	0·582
4	0·2704	0·8285	0·326	0·1982	0·8208	0·241	0·2441	0·8108	0·301
5	0·2200	1·2076	0·182	0·1639	1·2000	0·137	0·2202	1·1824	0·186
$\sum_{n=1}^{5}$	$2·3499 \times 10^{-3}$		$12·789 \times 10^{-3}$	$1·6754 \times 10^{-3}$	—	$9·010 \times 10^{-3}$	$1·8703 \times 10^{-4}$	—	$9·606 \times 10^{-4}$

Several noticeable cases are revealed as follows. (i) Let $X_0 = 0$ in equation (3), then equation (3) yields Nusselt number for heat flux distribution which varies from the initial heated position. (ii) Let $X_0 \to \infty$, then equation (3) yields Nusselt numbers for the case that heat flux changes from fully developed situation which is attained with uniform heat flux. (iii) Especially let $Z \to \infty$, then equation (3) is expected to give the Nusselt numbers for the asymptotic or fully developed situation if that situation exists. (iv) And let $F(Z) = 1$ or $H(Z) = 0$, equation (3) gives Nusselt number Nu_H for uniform heat flux, which is

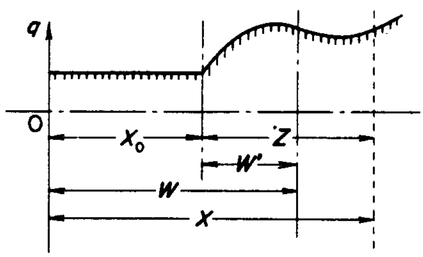

FIG. 2. Dimensionless axial distance.

$$\frac{1}{Nu_H} = \sum_{n=1}^{\infty} B_n[1 - \exp\{-C_n(X_0 + Z)\}]. \quad (4)$$

The results for a few simple heat flux distributions are shown in Table 2. Nusselt number for large Z enough to satisfy the relation $\exp(-C_n Z) \ll 1$, is represented with the subscript "0" as Nu_0 in Table 2.

Consequently $Nu_0 \equiv Nu_{fd}$ for the heat flux distribution which can bring about the fully developed situation.

THE CONVERGENCY OF THE ANALYTICAL SOLUTIONS

Since the thermal-entry-solutions are superposed to construct a solution for arbitrary heat flux or wall temperature distribution, the nature of the convergency of the former affects that of the superposed solution. There follows the investigation on the convergency of the analytical solutions under both of the boundary conditions. The Nusselt number for uniform heat flux is evaluated by equation (4). The fully developed Nusselt number, well known to exist in this case, reads clearly $Nu_{H,fd} = 1/\sum_{n=1}^{\infty} B_n$. The sum of the first five terms of B_n gives $\sum_{n=1}^{5} B_n = 0{\cdot}004219$ for $Pr = 0{\cdot}7$ and $Re = 50000$, as shown in Table 1. Hence $Nu_{H,fd} = 237$. This value of $Nu_{H,fd}$ greatly differs from the existing experimental values or the calculated value indicated at the later section. The higher the terms of B_n are taken beyond the first five, the more reasonable the value of the fully developed Nusselt number calculated by the sum of B_n becomes. But the convergency of B_n is so poor as shown in Table 1 that the addition of a few higher terms cannot be expected to predict the satisfactory fully developed Nusselt number. Consider the uniform wall temperature case in contrast with the uniform heat flux case. Under these boundary conditions Sleicher and Tribus [4] have given the thermal-entry-solution for turbulent flow in a tube. The result is that the Nusselt number Nu_T for uniform temperature is evaluated by

$$Nu_T = \sum_{n=1}^{\infty} A_n \exp\left\{-\left(\frac{2\lambda_n^2}{Re\,Pr}\right) Z\right\} \Big/ 2 \sum_{n=1}^{\infty} \frac{A_n}{\lambda_n^2} \exp\left\{-\left(\frac{2\lambda_n^2}{Re\,Pr}\right) Z\right\}. \quad (5)$$

Hence the fully developed Nusselt number depends on the first eigen-value alone, that is $Nu_{T,fd} = \lambda_1^2/2$. Values of A_n and λ_n^2 read from the graphical presentations [4] are reproduced for $Pr = 0{\cdot}718$ and $Re = 50000$ in Table 3. The Nusselt numbers Nu_H and Nu_T calculated by equations (4) and (5) respectively are shown in Fig. 3, where the symbol $n = 3$ or $n = 5$ represents the numbers of the terms used in the calculation. The result that $Nu_{H,fd}$ is smaller than $Nu_{T,fd}$ is considered to be mainly caused by the use of the different expressions for the

Table 2. Calculating equation

	(a)	(b)
$q = q_0F(Z)$	$q_0(1 + \alpha Z)$ 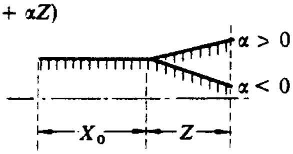	$q_0\{1 + b(1 - e^{\alpha Z})\}$ 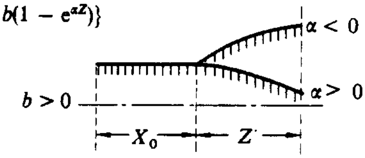
$\frac{1}{Nu}$	$\frac{1}{1 + \alpha Z}\left[\frac{1}{Nu_H} - \alpha\sum\frac{B_n}{C_n}(1 - C_nZ - e^{-C_nZ})\right]$	$\frac{1}{1 + b(1 - e^{\alpha Z})}\left[\frac{1}{Nu_H} + b\sum B_n\left\{1 - \frac{C_n}{\alpha + C_n} \times e^{\alpha Z} - \frac{\alpha}{\alpha + C_n}e^{-C_nZ}\right\}\right]$
$\frac{1}{Nu_H} - \frac{1}{Nu}$	$\frac{\alpha}{1 + \alpha Z}\sum\frac{B_n}{C_n}\left[1 - \frac{C_nZ\,e^{-C_nX_0} + 1}{e^{C_nZ}}\right]$	$\frac{-\alpha b\,e^{\alpha Z}}{1 + b(1 - e^{\alpha Z})}\sum B_n\left[\frac{1}{\alpha + C_n}\{1 - e^{-(\alpha + C_n)Z}\} + \frac{1}{\alpha}e^{-C_nX_0}\{e^{-(\alpha + C_n)Z} - e^{-C_nZ}\}\right]$
$X_0 = 0$	$\frac{\alpha}{1 + \alpha Z}\sum\frac{B_n}{C_n}\left[1 - \frac{C_nZ + 1}{e^{C_nZ}}\right]$	$\frac{-\alpha b\,e^{\alpha Z}}{1 + b(1 - e^{\alpha Z})}\left[\sum\frac{B_n}{\alpha + C_n} - \sum B_n\left\{\frac{1}{\alpha}e^{-C_nZ} - \frac{C_n}{\alpha(\alpha + C_n)}e^{-(\alpha + C_n)Z}\right\}\right]$
$X_0 = \infty$	$\frac{\alpha}{1 + \alpha Z}\sum\frac{B_n}{C_n}(1 - e^{-C_nZ})$	$\frac{-\alpha b\,e^{\alpha Z}}{1 + b(1 - e^{\alpha Z})}\sum\frac{B_n}{\alpha + C_n}\{1 - e^{-(\alpha + C_n)Z}\}$
$\frac{1}{Nu_{H,fd}} - \frac{1}{Nu_0}$	$\sim\frac{\alpha}{1 + \alpha Z}\sum\frac{B_n}{C_n}$	$\sim\frac{-\alpha b\,e^{\alpha Z}}{1 + b(1 - e^{\alpha Z})}\sum\frac{B_n}{\alpha + C_n}$†

Symbol $\sum$ represents summation of terms up to infinity.
† $\alpha > 0$ or $|\alpha| < C_n$. § $\alpha < C_n$.
‡ In this case $Nu_0 \equiv Nu_{fd}$.

of Nusselt numbers

(b′)	(c)
$q_0\,\mathrm{e}^{\alpha Z}$ 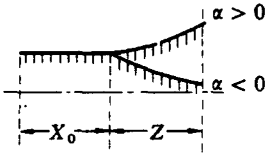	$q_0(1 + b \sin \alpha Z)$· 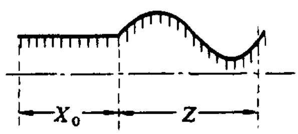
$\frac{1}{\mathrm{e}^{\alpha Z}} \sum B_n \left\{ \frac{C_n}{\alpha + C_n} \mathrm{e}^{\alpha Z} + \frac{\alpha}{\alpha + C_n} \times \mathrm{e}^{-C_n Z} - \mathrm{e}^{-C_n(X_0 + Z)} \right\}$	$\frac{1}{1 + b \sin \alpha Z} \left[\frac{1}{Nu_H} + \sum \frac{B_n}{1 + (\alpha/C_n)^2} \times \left(\sin \alpha Z - \frac{\alpha}{C_n} \cos \alpha Z + \frac{\alpha}{C_n} \mathrm{e}^{-C_n Z} \right) \right]$
$\alpha \sum B_n \left[\frac{1}{\alpha + C_n} \{1 - \mathrm{e}^{-(\alpha + C_n) Z}\} + \frac{1}{\alpha} \mathrm{e}^{-C_n(X_0 + Z)} (\mathrm{e}^{-\alpha Z} - 1) \right]$	$\frac{\alpha b \cos \alpha Z}{1 + b \sin \alpha Z} \left[\sum \frac{B_n C_n}{\alpha^2 + C_n^2} \left(1 + \frac{\alpha}{C_n} \tan \alpha Z \right) - \sum B_n \frac{\mathrm{e}^{-C_n Z}}{\cos \alpha Z} \left(\frac{C_n}{\alpha^2 + C_n^2} + \frac{\mathrm{e}^{-C_n X_0}}{\alpha} \sin \alpha Z \right) \right]$
$\alpha \left[\sum \frac{B_n}{\alpha + C_n} - \sum B_n \left\{ \frac{1}{\alpha} \mathrm{e}^{-C_n Z} - \frac{C_n}{\alpha(\alpha + C_n)} \mathrm{e}^{-(\alpha + C_n) Z} \right\} \right]$	$\frac{\alpha b \cos \alpha Z}{1 + b \sin \alpha Z} \left[\sum \frac{B_n C_n}{\alpha^2 + C_n^2} \left(1 + \frac{\alpha}{C_n} \tan \alpha Z \right) - \sum B_n \frac{\mathrm{e}^{-C_n Z}}{\cos \alpha Z} \left(\frac{C_n}{\alpha^2 + C_n^2} + \frac{1}{\alpha} \sin \alpha Z \right) \right]$
$\alpha \sum \frac{B_n}{\alpha + C_n} \{1 - \mathrm{e}^{-(\alpha + C_n) Z}\}$	$\frac{\alpha b \cos \alpha Z}{1 + b \sin \alpha Z} \left[\sum \frac{B_n C_n}{\alpha^2 + C_n^2} \left(1 + \frac{\alpha}{C_n} \tan \alpha Z - \frac{\mathrm{e}^{-C_n Z}}{\cos \alpha Z} \right) \right]$
$\sim \alpha \sum \frac{B_n}{\alpha + C_n}$†‡	$\sim \frac{\alpha b \cos \alpha Z}{1 + b \sin \alpha Z} \sum \frac{B_n C_n}{\alpha^2 + C_n^2} \left(1 + \frac{\alpha}{C_n} \tan \alpha Z \right)$§

eddy diffusivity for heat. The fully developed Nusselt number for uniform wall temperature calculated with the same expressions of the velocity profile and eddy diffusivity for heat as those used in the case of the uniform heat flux,

Table 3. Listing of A_n and λ_n^2 (reproduced from reference [4])

$Re = 50000$, $Pr = 0.718$		
n	A_n	λ_n^2
1	30·0	236
2	5·78	2640
3	3·74	7440

designated as $Nu^*_{T,fd}$ in Fig. 3, is slightly smaller than $Nu_{H,fd}$. In the case of the uniform wall temperature, the first three terms of the infinite series in equation (5) give the satisfying Nusselt number and the thermal-entry-solution has very good convergency. The superposed solution for arbitrary wall temperature distribution also

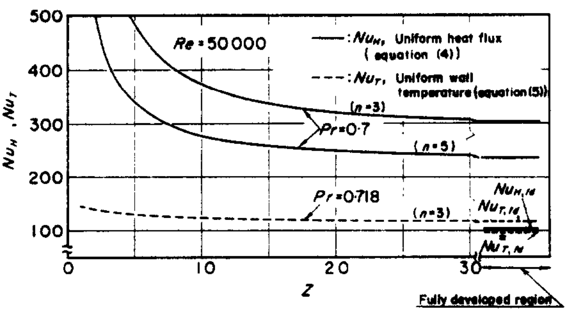

FIG. 3. Nusselt number variations for uniform heat flux and uniform wall temperature distributions.

shows good convergency and the corresponding Nusselt number can be reasonably evaluated at most with the first three or four eigen-values and corresponding coefficients.

It is noted here that the difference in the boundary conditions strikingly affects the nature of convergency of the superposed solution. Since the relation between the eigen values and corresponding coefficients for the uniform heat flux and those for the uniform wall temperature has been established [5], the poor convergency of the superposed solution is concluded to be inevitable for the problem of arbitrary heat flux distribution.

APPROXIMATE METHOD FOR THE CALCULATION OF NUSSELT NUMBER

The poor convergent nature of the superposed solution for arbitrary heat flux distribution cannot be settled effectively by means of the increase of the terms of the infinite series. Consequently, another means should be worked out as follows.

Various sums of the infinite series which appear in the calculating equation of Nusselt number are divided into two groups by the dependency on the axial coordinate. Each term of the first group consists of B_n and C_n, and accordingly the sums of the infinite series are independent of the axial coordinate Z. On the other hand each term of the second group contains the exponential function $\exp(-C_n Z)$, and therefore the sums depend on the axial coordinate Z. Now the convergencies of these two groups of the infinite series are examined. The case of $Pr = 0.7$ and $Re = 50000$ is taken as an example. The convergent nature of B_n has been mentioned in the previous section. As the series C_n are increasing ones, the series B_n/C_n have relatively better convergency than B_n do, which is shown in Table 1, but the neglection of the higher terms gives rise to considerable error in the calculated Nusselt number. On the other hand the convergencies of the series $B_n \exp(-C_n Z)$ and the series $(B_n/C_n) \exp(-C_n Z)$ are shown in Figs. 4 and 5 respectively. It is clear from Figs. 4 and 5 that for $Z > 3$ the neglection of the higher terms beyond the first five has no appreciable effect on the total sums of the infinite series containing the exponential function $\exp(-C_n Z)$. Hence the error in the calculation of Nusselt number is chiefly caused by dropping the higher terms in the evaluation of such fixed sums of the first group as $\sum_{n=1}^{\infty} B_n$ and and $\sum_{n=1}^{\infty} (B_n/C_n)$. In the evaluation of such sums

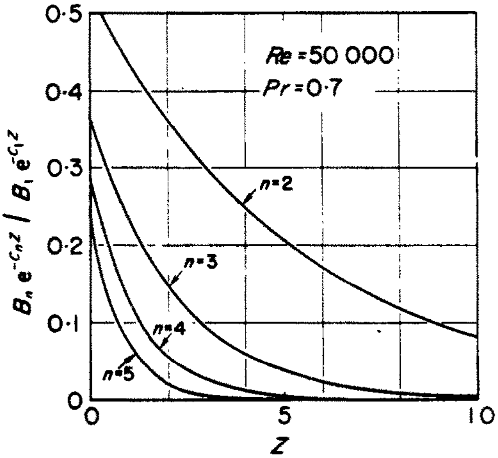

FIG. 4. Convergency of $B_n \exp(-C_n Z)$.

of the second group as $\sum_{n=1}^{\infty} B_n \exp(-C_n Z)$ and $\sum_{n=1}^{\infty} (B_n/C_n) \exp(-C_n Z)$, the same kind of error is negligibly small except for Z near zero provided that the first five terms of B_n and C_n are used. In conclusion the accurate evaluation of the sums of the first group makes it possible to predict reasonable Nusselt numbers except in the region of extremely small Z where the poor convergency of the infinite series of the second group gives rise to the inevitable error. For example, in equation (4), divide formally the

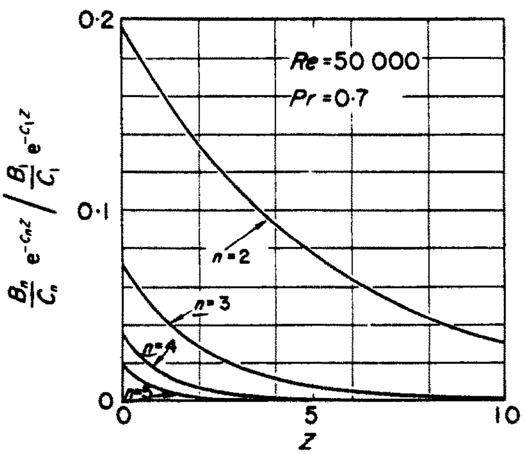

FIG. 5. Convergency of $(B_n/C_n) \exp(-C_n Z)$.

sums of the right-hand side into two groups as

$$\frac{1}{Nu_H} = \sum_{n=1}^{\infty} B_n - \sum_{n=1}^{\infty} B_n \exp(-C_n Z). \quad (6)$$

Then accurate Nusselt number can be calculated for $Z > 3$ with the first five terms of B_n and C_n provided that $\sum_{n=1}^{\infty} B_n$ is fixed beforehand.

The key point of the proposed approximate calculating method is the prior evaluation of such first group sums as $\sum_{n=1}^{\infty} B_n$ and $\sum_{n=1}^{\infty} (B_n/C_n)$ with poor convergent nature. The details of the evaluating method and results will be shown in the later section.

ANALYTICAL CONSIDERATION ON FULLY DEVELOPED SITUATION

For the two conditions, uniform heat flux and uniform wall temperature, it has been well known that the fully developed situations are reached beyond the thermal entrance region and the Nusselt numbers take the fixed values different from each other. In addition to these two cases, there can be mentioned heat flux or wall temperature distributions which give formally fixed Nusselt numbers when axial distance Z tends to infinity in the calculating equation of Nusselt number $Nu(Z)$. Hitherto in these cases, it has been considered that the fully developed situation exists and the corresponding fixed Nusselt number has been called the fully developed one. Even if such conditions are formally satisfied by the mathematical operation of limit in the calculating equation, it does not necessarily mean the temperature profile reaches the fully developed one. To clear the conditions for the existence of the fully developed situation, there follows the theoretical analysis on what cases the fully developed situation with a generalized temperature profile invariant in the direction of flow is obtained when prescribed axially varying heat flux is given. Hence the exponentially varying heat flux is revealed to be only the distribution which realizes the fully developed situation and fully developed Nusselt numbers are calculated to evaluate the sums

$$\sum_{n=1}^{\infty} B_n \quad \text{and} \quad \sum_{n=1}^{\infty} (B_n/C_n).$$

ANALYSIS

The system considered is that of incompressible fluid of constant properties flowing in a tube with fully developed velocity profile. The coordinate system is shown in Fig. 1.

The energy equation describing the problem is to be expressed as

$$u\frac{\partial T}{\partial x} = \frac{1}{r}\frac{\partial}{\partial r}\left[r(a + \varepsilon_H)\frac{\partial T}{\partial r}\right] \tag{7}$$

where T is fluid temperature, x axial coordinate, r radial coordinate, u flow velocity, a thermal diffusivity and ε_H eddy diffusivity for heat. Substitution of the following dimensionless variables into equation (7) yields

$$s = \frac{r}{r_0}, \quad z = \frac{x}{2r_0RePr}, \quad v = \frac{u}{u_a},$$

$$g = 1 + \frac{\varepsilon_H}{a},$$

$$v\frac{\partial T}{\partial z} = \frac{4}{s}\frac{\partial}{\partial s}\left(sg\frac{\partial T}{\partial s}\right) \tag{8}$$

with boundary conditions

$$\frac{\partial T}{\partial s} = 0 \quad \text{at} \quad s = 0, \qquad \frac{\partial T}{\partial s} = \frac{r_0 q}{k} \quad \text{at} \quad s = 1. \tag{9}$$

Suppose both the velocity and the temperature profiles are fully developed, there exists a generalized temperature profile that is invariant with tube length. The statement that this profile is invariant with x can be expressed as [6]

$$\frac{\partial}{\partial x}\left(\frac{T_w - T}{T_w - T_m}\right) = 0 \tag{10}$$

where the subscript w refers to the value at wall and the subscript m, the mixed mean value. Under the fully developed situation, the heat-transfer coefficient is constant along the tube length and therefore equation (10) can be rewritten as

$$\frac{\partial}{\partial x}\left(\frac{T_w - T}{q}\right) = 0. \tag{11}$$

Hence the dimensionless temperature θ that is defined in equation (12) is a function of s only.

$$\theta = \frac{T_w - T}{\dfrac{2r_0q}{k}}. \tag{12}$$

Take the mixed mean value of equation (12), and the heat balance between heat flux and the mixed mean temperature rise,

$$T_w - T_m = \theta_m\frac{2r_0q}{k} \tag{13}$$

$$\frac{\mathrm{d}T_m}{\mathrm{d}z} = \frac{8r_0q}{k}. \tag{14}$$

Thus, substituting equation (12) in equation (8) and (9),

$$v\left[(\theta - \theta_m)\frac{1}{q}\frac{\mathrm{d}q}{\mathrm{d}z} - 4\right] = \frac{4}{s}\frac{\mathrm{d}}{\mathrm{d}s}\left(sg\frac{\mathrm{d}\theta}{\mathrm{d}s}\right) \tag{15}$$

mixed mean temperature rise.

$$\frac{\mathrm{d}\theta}{\mathrm{d}s} = 0 \quad \text{at} \quad s = 0, \qquad \frac{\mathrm{d}\theta}{\mathrm{d}s} = -\frac{1}{2} \quad \text{at} \quad s = 1. \tag{16}$$

In order that θ may be obtained as the function of s alone by the solution of equation (15), heat flux should meet the following requirement,

$$\frac{1}{q}\frac{\mathrm{d}q}{\mathrm{d}z} = \eta$$

or

$$q = C\exp(\eta z) = C\exp\left(\eta\frac{x}{2r_0RePr}\right)$$

$$= C\exp\left(\alpha\frac{x}{2r_0}\right), \tag{17}$$

where η, α and C are constants and $\eta \equiv \alpha Re\,Pr$. Defining $\varphi = \theta_m - \theta$, equations (15) and (16) take the following forms.

$$v(4 + \eta\varphi) = \frac{4}{s}\frac{d}{ds}\left(sg\frac{d\varphi}{ds}\right) \qquad (18)$$

$$\frac{d\varphi}{ds} = 0 \quad \text{at} \quad s = 0, \qquad \frac{d\varphi}{ds} = \frac{1}{2} \quad \text{at} \quad s = 1. \qquad (19)$$

Thus, it is only when the heat flux varies exponentially along the tube length that there exists beyond the thermal entry region the fully developed situation with a generalized temperature profile which is invariant in the direction of flow. The fully developed temperature profile is given by the solution of equation (18) with the boundary conditions (19) and depends on the parameter η. The Nusselt number is evaluated from equation (20).

$$Nu_{fd} = \frac{q}{T_w - T_m} \times \frac{2r_0}{k} = \frac{1}{\theta_m} = \frac{1}{\varphi_w}. \qquad (20)$$

Prior to solving equation (18), the wall temperature and the mixed mean temperature variations along the tube length are examined to find the conditions on the wall temperature distribution which can give rise to the fully developed situation. From equations (13, 14, 17) the first and the second derivatives of the wall and the mixed mean temperatures are deduced as follows.

$$\left.\begin{aligned} &\frac{dT_m}{dz} = \frac{8r_0 q}{k}, \qquad \frac{d^2T_m}{dz^2} = \frac{8r_0}{k}\eta q, \\ &\frac{dT_w}{dz} = \frac{2r_0}{k}(4 + \eta\theta_m)\,q, \\ &\frac{d^2T_w}{dz^2} = \frac{2r_0}{k}(4 + \eta\theta_m)\,\eta q. \end{aligned}\right\} \qquad (21)$$

By referring to the signs of these derivatives, the temperature variations are shown in Fig. 6. It is clear that the temperature variations to realize the fully developed situation are classified into the five typical patterns depending on the values of the parameter η. The uniform heat flux case corresponds to $\eta = 0$, while the uniform wall temperature case corresponds to $\eta = -4Nu_{T,fd}$. Both boundary conditions, in which the existence of the fully developed situation has been well known, are included as the special cases in the exponential heat flux distribution.

To carry out the solution of equation (18), the variations of v and g with s must be given. Since there is no various selection of v and g for laminar flow where

$$v = 2(1 - s^2), \qquad g = 1$$

it is convenient to check the present analysis with the available results by other investigators. For turbulent flow the velocity profile is taken from Deissler's analysis [7], which is expressed as

$$0 \leqslant y^+ \leqslant 26$$

$$\frac{du^+}{dy^+} = \frac{1}{1 + (0{\cdot}124)^2 u^+ y^+ [1 - \exp\{-(0{\cdot}124)^2 u^+ y^+\}]}$$

$$26 < y^+ \qquad u^+ = \frac{1}{0{\cdot}36}\ln\left(\frac{y^+}{26}\right) + 12{\cdot}8493. \qquad (22)$$

The eddy diffusivity for heat is assumed to be equal to that for momentum.

Numerical integration of equation (18) subject to the boundary conditions (19) are carried out [8] by Runge–Kutta method on the digital computer (OKITAK-5090) in Kyushu University.

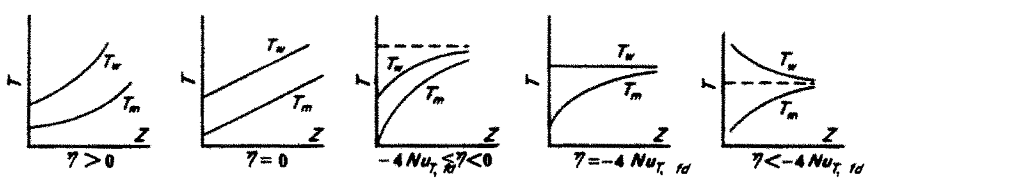

FIG. 6. Temperature variations with tube length.

NUMERICAL RESULTS

(i) *Laminar flow.* A plot of the fully developed Nusselt number Nu_{fd} is given as a function of η in Fig. 7. Figure 8 shows the radial temperature profiles. By putting $\eta = 0$ for uniform heat flux, equation (18) is solved analytically and the corresponding fully developed Nusselt pumber

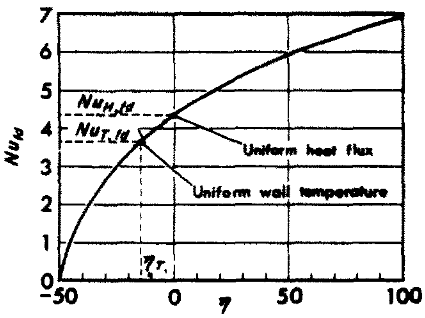

FIG. 7. Calculated Nusselt numbers (laminar flow).

$Nu_{H,fd} = 4{\cdot}364$. The fully developed Nusselt number $Nu_{T,fd}$ and the parameter η_T for uniform wall temperature satisfy the relation $\eta_T + 4Nu_{T,fd} = 0$, which gives $Nu_{T,fd} = 3{\cdot}658$ and $\eta_T = -14{\cdot}632$. This value of $Nu_{T,fd}$ is in accordance with that [9] obtained by a successive approximation of the energy equation under uniform wall temperature boundary conditions. The corresponding temperature profile shown in Fig. 8 is in excellent agreement with that [10] presented by Jakob. Although negative values of η satisfy the fully developed conditions, the temperature profile oscillates with radial direction when η is smaller than the negative limiting value η_0. The absolute value of η_0 is equal to the first eigen value of the energy equation for uniform heat flux. The fully developed Nusselt number increases monotonically with the increase of η, provided that $\eta > \eta_0$. The change in temperature between wall and fluid is more localized in the region adjacent to the wall and temperature profile becomes flatter in the center region with the increase of η, provided that $\eta > \eta_0$.

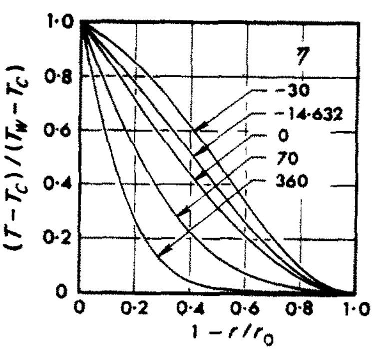

FIG. 8. Radial temperature profiles (laminar flow).

(ii) *Turbulent flow.* The fully developed Nusselt numbers are presented in Table 4. The radial temperature profiles for Reynolds number of 50000 and Prandtl number of 0·7 are shown in Fig. 9. The same remarks about laminar flow also hold true in the case of turbulent flow.

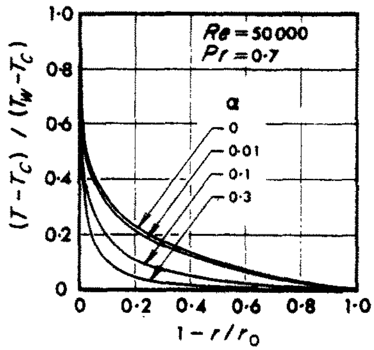

FIG. 9. Radial temperature profiles.

EVALUATION OF THE SUMS $\sum_{n=1}^{\infty} B_n$ AND $\sum_{n=1}^{\infty} (B_n/C_n)$

There are shown as follows the method and the results of the evaluation of the sums $\sum_{n=1}^{\infty} B_n$ and $\sum_{n=1}^{\infty} (B_n/C_n)$ from the calculating results in the foregoing section. A relation shown in Table 1 exists between the fully developed Nusselt numbers for the uniform heat flux and the exponentially varying heat flux. That is

$$\frac{1}{Nu_{H,fd}} - \frac{1}{Nu_{fd}} = \alpha \sum_{n=1}^{\infty} \frac{B_n}{C_n + \alpha}. \qquad (23)$$

Table 4. Calculated fully developed Nusselt numbers

α	$Re = 50000$			$Re = 100000$		
	$Pr = 0{\cdot}7$	$Pr = 1{\cdot}0$	$Pr = 10$	$Pr = 0{\cdot}7$	$Pr = 1{\cdot}0$	$Pr = 10$
−0·05	86·5	108·0	361·2	143·6	181·6	646·0
−0·01	99·7	122·6	379·0	167·7	208·6	680·3
0	102·1	125·2	382·0	171·8	213·2	685·7
0·01	104·2	127·5	384·7	175·4	217·2	690·4
0·05	111·2	135·1	393·3	187·1	230·0	704·8
0·1	117·8	142·1	401·3	197·8	241·6	717·7

As $Nu_{H,fd} = 1/\sum_{n=1}^{\infty} B_n$, equation (23) reads

$$\frac{1}{Nu_{fd}} = \sum_{n=1}^{\infty} B_n - \alpha \sum_{n=1}^{\infty} \frac{B_n}{C_n + \alpha}. \qquad (24)$$

Let $\alpha = 0$ in equation (24)

$$\sum_{n=1}^{\infty} B_n = \left(\frac{1}{Nu_{fd}}\right)_{\alpha=0}. \qquad (25)$$

After differentiating equation (24) with respect to α, let α tend to zero

$$\sum_{n=1}^{\infty} \frac{B_n}{C_n} = \lim_{\alpha \to 0} \left[\frac{1}{(Nu_{fd})^2} \times \frac{dNu_{fd}}{d\alpha}\right]. \qquad (26)$$

Consequently the values of $\sum_{n=1}^{\infty} B_n$ and $\sum_{n=1}^{\infty} (B_n/C_n)$ may be evaluated from the ordinate and the gradient at $\alpha = 0$ in the $Nu_{fd} - \alpha$ curves shown in Fig. 10. The results are given in Table 5.

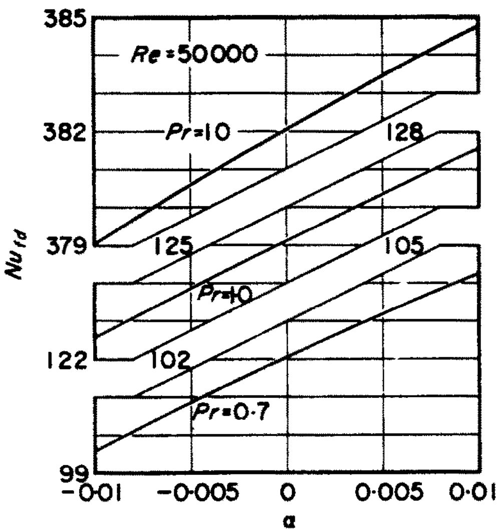

FIG. 10. Fully developed Nusselt numbers as a function of the parameter α.

EXPERIMENTAL APPARATUS AND PROCEDURE

The apparatus employed in the experiment is shown diagrammatically in Fig. 11. Air from the atmosphere is flowed by the fan through the flow meter into the mixing chamber. After mixed enough there, air flows through the straight tubes which are constructed from the velocity developing section and the heated section. The velocity developing tube has an I.D. of 21·2 mm and a length of about 1000 mm (47 d). For the Reynolds number under experiment ($Re = 50000$), the velocity profile is considered to be fully developed at the exit of the velocity developing tube. Then there follows the 1000-mm length of heated tube with the same I.D. as the velocity developing tube. To keep off axial heat loss, both ends of the heated tube are insulated from their neighbours by the insulating ring made of Teflon and finished smoothly inside not to disturb the flow field. The mixing chamber, the velocity developing tube and the heated tube are lagged with a 50-mm thickness of performed glass fibre insulation. The heated tube is the drawn stainless steel tube (SUS 27) and has an I.D. of 21·2 mm and a maximum O.D. of 33·4 mm. Heating is

Table 5. Listing of the sums, $\sum_{n=1}^{\infty} B_n$ *and* $\sum_{n=1}^{\infty} (B_n/C_n)$

	$Re = 50000$			$Re = 100000$		
	$Pr = 0{\cdot}7$	$Pr = 1{\cdot}0$	$Pr = 10$	$Pr = 0{\cdot}7$	$Pr = 1{\cdot}0$	$Pr = 10$
$\sum_{n=1}^{\infty} B_n$	$9{\cdot}799 \times 10^{-3}$	$7{\cdot}990 \times 10^{-3}$	$2{\cdot}618 \times 10^{-3}$	$5{\cdot}822 \times 10^{-3}$	$4{\cdot}691 \times 10^{-3}$	$1{\cdot}458 \times 10^{-3}$
$\sum_{n=1}^{\infty} \frac{B_n}{C_n}$	$21{\cdot}57 \times 10^{-3}$	$15{\cdot}69 \times 10^{-3}$	$1{\cdot}929 \times 10^{-3}$	$13{\cdot}08 \times 10^{-3}$	$9{\cdot}357 \times 10^{-3}$	$1{\cdot}057 \times 10^{-3}$

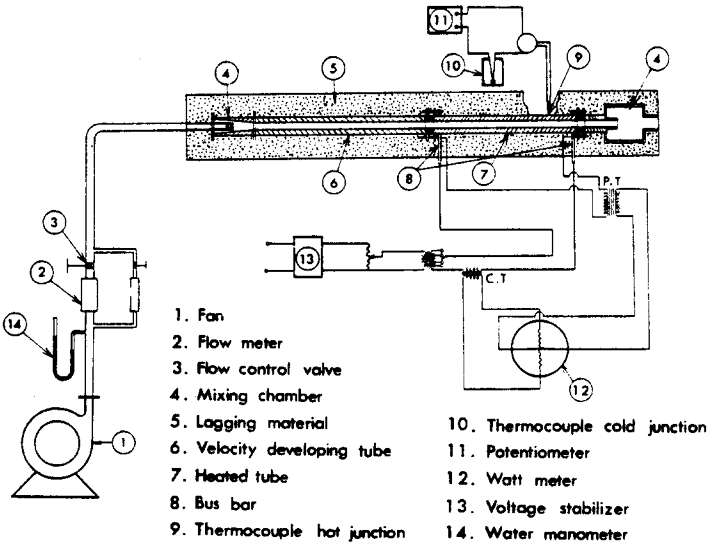

FIG. 11. Experimental apparatus.

accomplished by passing low voltage a.c. (1·5 ~ 2 V) through the length of the heated tube. The outer diameter was lathed in the prescribed size along the tube so that the heat flux could be distributed in a prescribed manner along its length. It is difficult to measure the heat generation at an arbitrary point under experiment, so the heat generation distribution per unit tube length was fixed along its length beforehand by measuring the voltage drop between each small section with a 8 mm in distance at a uniform temperature. The air inlet temperature was measured at the mixing chamber and at the point 15 d downstream from it. The outer wall temperatures of the heated tube were measured by copper–constantan thermocouples soldered at intervals of nearly the same distance (40 mm) along the tube surface.

The experiments were carried out with air as the flowing fluid for Reynolds number of 50000. Five to eight hours were allowed for the steady conditions and the usual duration of one measurement was a half to one hour.

Experimental data werc correlated by the Nusselt number

$$Nu = \frac{hd}{k} = \frac{q}{T_w - T_m} \times \frac{d}{k}$$

where h is heat-transfer coefficient and k thermal conductivity of the fluid which is evaluated at the mean film temperature $\frac{1}{2}(T_w + T_m)$. The thermocouple readings measuring the tube outer wall temperature were corrected for the drop across the wall.

Heat flux was calculated by

$$q = \frac{1}{\pi d}\left[Q_E \frac{e(x)}{E(x_L)} - \pi DK(T_w - T_R) + \frac{\pi}{4}(D^2 - d^2)\, k_s \frac{d^2 T_w}{dx^2}\right] \tag{27}$$

where Q_E is total heat generation, $e(x)$ heat generation distribution per unit tube length corrected for the wall temperature variation along the tube, $E(x) = \int_0^x e(x)\,dx$, x_L total length of the heated tube, D tube outer diameter, K overall coefficient of heat transfer based on T_w and T_R, T_R ambient temperature, k_s thermal conductivity of the heated tube. K was measured to be $K = 1{\cdot}54$ kcal/m^{2}h°C with the same tube and lagging as that used in the experiment.

The mixed mean temperature of the fluid was calculated as the sum of the measured inlet temperature and the temperature rise corresponding to the heat input (corrected for radial heat loss to the atmosphere and axial conduction in the tube wall) from the wall up to the position under consideration. Then

$$T_m = T_{in} + \frac{1}{Gc_p\gamma}$$
$$\times \left[Q_E \frac{E(x)}{E(x_L)} - \pi DK \int_0^x (T_w - T_R)\,\mathrm{d}x + \frac{\pi}{4}(D^2 - d^2)\,k_s \frac{\mathrm{d}T_w}{\mathrm{d}x}\bigg|_0^x \right] \qquad (28)$$

where T_{in} is inlet air temperature, G volumetric flow rate, c_p specific heat of air and γ specific weight of air. The derivatives $\mathrm{d}T_w/\mathrm{d}x$ and $\mathrm{d}^2T_w/\mathrm{d}x^2$ in equations (27) and (28) were found by graphical differentiation or polinominal approximation of the measured wall temperature distribution.

EXPERIMENTAL AND CALCULATED RESULTS

Experimental data taken under the conditions of uniform heat flux are compared with the calculated results in Fig. 12. Calculated curve is obtained for $Pr = 0{\cdot}7$ and $Re = 50000$ by equation (6) with aid of the sum $\sum_{n=1}^{\infty} B_n$ in Table 5 and the first five terms of $B_n \exp(-C_n Z)$. The corresponding fully developed Nusselt numbers are shown in Fig. 13, where calculated curve presents the results from Table 4.

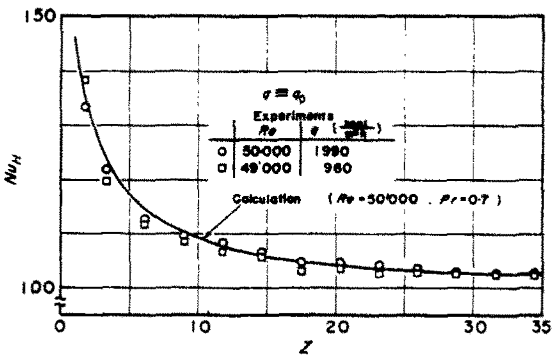

FIG. 12. Nusselt number variation for uniform heat flux.

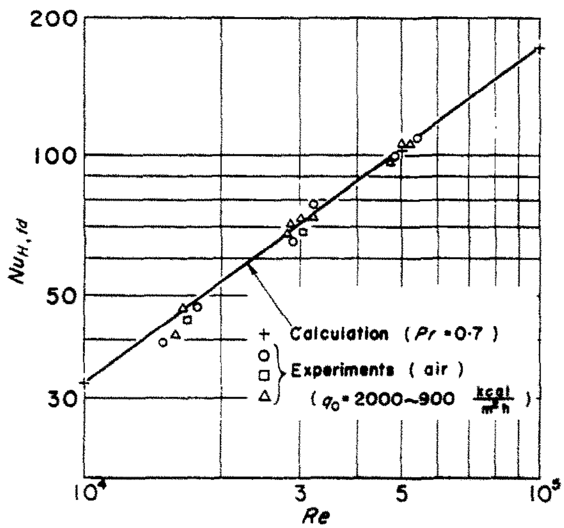

FIG. 13. Fully developed Nusselt number for uniform heat flux.

Figure 14 reveals the results for the rectilinear heat flux increase from the point $x/d = 20$ with the uniform heat flux upstream of that point. The calculating equation is obtained by substituting $X_0 = 20$ in the equation at column (a) in Table 2. The solid curve is obtained by the approximate method with the fixed sums of

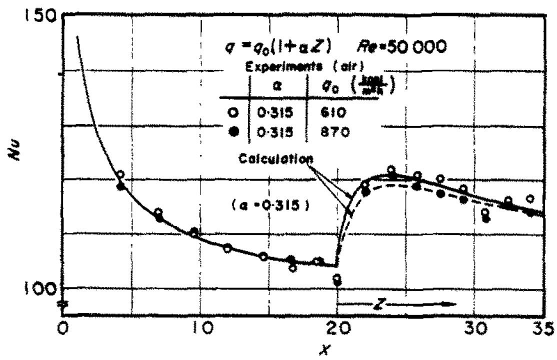

FIG. 14. Nusselt number variation for rectilinearly varying heat flux.

$\sum_{n=1}^{\infty} B_n$ and $\sum_{n=1}^{\infty} (B_n/C_n)$ in Table 5 as the first group sums and the first five terms of B_n and C_n for the evaluation of the second group sums. The maximum error accompanied to this method is 0·1 per cent in Nusselt number. The dotted curve represents the results by means of the same calculating method as that for the solid curve with exception that $\sum_{n=1}^{5} (B_n/C_n)$ is used instead of $\sum_{n=1}^{\infty} (B_n/C_n)$. The appreciable deviation of the dotted curve from the solid one originates in the neglection of the higher terms of B_n/C_n and decreases as Z increases. The Nusselt numbers for rectilinear heat flux distributions are shown in Fig. 15. Calculating

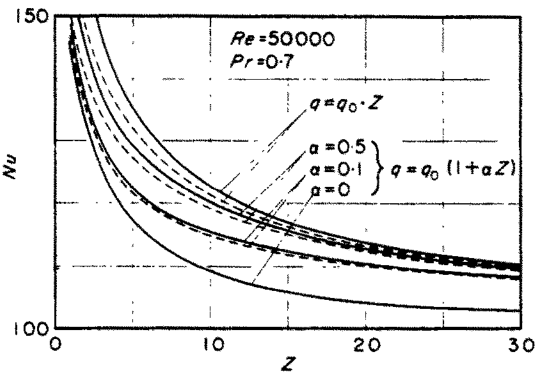

FIG. 15. Nusselt number variations for rectilinearly varying heat flux.

equation is obtained by putting $X_0 = 0$ in the equation at column (a) in Table 2, which reads

$$\frac{1}{Nu_H} - \frac{1}{Nu} = \frac{\alpha}{1 + \alpha Z} \times \left[\sum_{n=1}^{\infty} \frac{B_n}{C_n} - \sum_{n=1}^{\infty} \frac{B_n}{C_n} \cdot \frac{C_n Z + 1}{\exp(C_n Z)}\right]. \tag{29}$$

The sums of the first group which appear in equation (29) are $\sum_{n=1}^{\infty} B_n$ in Nu_H and $\sum_{n=1}^{\infty} (B_n/C_n)$. The solid curves in Fig. 15 represent the results by the approximate method with $\sum_{n=1}^{\infty} B_n$ and $\sum_{n=1}^{\infty} (B_n/C_n)$ in Table 5 and the first five terms for the evaluation of the second group sums. The maximum error at $Z = 3$ is 0·2 per cent in Nusselt number. The dotted curve corresponding to each solid curve represents the results by the same method with the only exception that $\sum_{n=1}^{5} (B_n/C_n)$ is used instead of $\sum_{n=1}^{\infty} (B_n/C_n)$. The difference between each two curves increases with the increase of α and with the decrease of Z.

As shown in Table 2

$$\lim_{Z \to \infty} Nu = Nu_{H,fd}.$$

This means that the denominator $(1 + \alpha Z)$ in equation (29) tends to infinity, that is, heat flux tends to infinity. This situation differs from the fully developed one because it can be realized only with the exponentially varying heat flux. In the region where the relation $\exp(-C_n Z) \ll 1$ is satisfied, the Nusselt number tends asymptotically to the curve

$$\left[\sum_{n=1}^{\infty} B_n + \frac{\alpha}{1 + \alpha Z} \sum_{n=1}^{\infty} \frac{B_n}{C_n}\right]^{-1}$$

which indicates gradual change in the direction of Z. Consequently in this region Nusselt number has different value from $Nu_{H,fd}$ and shows the quasi-asymptotic character. In this quasi-asymptotic situation Nusselt numbers are slightly affected by the parameter α. The Nusselt number for linear heat flux distribution is independent of the gradient and greater than that for other rectilinear heat fluxes.

Figure 16 reveals the Nusselt numbers for the exponentially varying heat flux distributions. The calculating equations are shown in column (b′) in Table 2. The calculated curve is obtained by the approximate method with the fixed sums and the first five terms for the evaluation the second group sums. The first group sums which appeared in the calculating equation are

$$\sum_{n=1}^{\infty} B_n \quad \text{and} \quad \sum_{n=1}^{\infty} \frac{B_n}{C_n + \alpha}.$$

The sum

$$\sum_{n=1}^{\infty} \frac{B_n}{C_n + \alpha}$$

is approximated by

$$\sum_{n=1}^{\infty} \frac{B_n}{C_n + \alpha} \cong \sum_{n=1}^{5} \frac{B_n}{C_n + \alpha} + \sum_{n=6}^{\infty} \frac{B_n}{C_n}$$

because each value of B_n and C_n is unknown for $n \geqslant 6$ but the relation $C_n \gg \alpha$ can be assumed for $n \geqslant 6$ ($C_6 \approx 1{\cdot}848$, $\alpha = 0{\cdot}07$ and $0{\cdot}01$). It is analytically proved already in this paper that the exponentially varying heat flux realizes the fully developed situation. And the experimental and the calculated results show the fully developed situation is reached with the shorter thermal-entry-length and the corresponding Nusselt number takes higher values as the parameter α increases. These facts are compatible with the results shown in Fig. 9, that is the change in temperature between wall and fluid is more localized in the region adjacent to the wall as the parameter α increases. The values of Nusselt number are affected sensitively by the parameter α in the case of the exponential heat flux distribution in contrast with the case of the rectilinear heat flux distribution, whose Nusselt numbers are not so sensible to the parameter α and take the values between the Nusselt number for the uniform heat flux and that for the linear heat flux distribution as shown in Fig. 15. Thus it should be noted that the shape of the heat flux distribution strongly influences the behaviour of the corresponding Nusselt number. The difference between the fully developed Nusselt numbers for exponentially varying heat flux and that for the uniform heat flux is expressed as a ratio of the latter in Fig. 17.

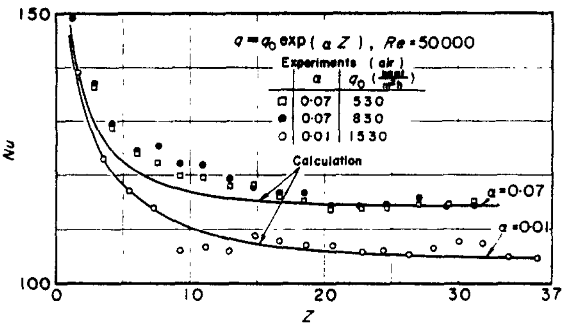

FIG. 16. Nusselt number variations for exponentially varying heat flux.

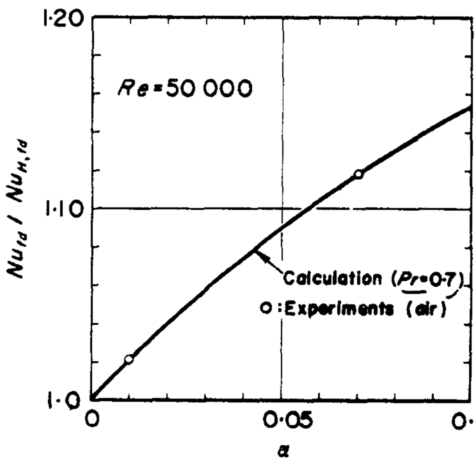

FIG. 17. Ratio of fully developed Nusselt number for exponentially varying heat flux to that for uniform heat flux.

Experimental results are deduced from those in Fig. 13 and 16 and the calculated curve represents the results in Table 4.

For the limited heat flux distributions and the particular fluid and Reynolds number, the calculated results by the approximate method are in better agreement with the experimental data except the region near the initial heated point ($Z < 3$). The correspondency or the deviation discerned in the region near the initial heated point is insignificant because the calculated results contain inevitable errors caused by the evaluation of the second group sums and the experimental results have errors caused by no support of the assumed heat flux distribution on account of the considerable axial heat flow.

CONCLUDING REMARKS

As for turbulent heat transfer in a tube with arbitrary heat flux distribution, the approximate method was proposed to correct the error caused by the poor convergency of the superposed solution and to predict reasonable Nusselt number. The essential point is that the sums of the first group infinite series constructed by the eigen-values and the corresponding coefficients can be fixed beforehand. Two kinds of the sums were calculated correctly from the fully developed Nusselt numbers. The calculated Nusselt number by the approximate method with the evaluated first group sums and with the first five eigen-values and corresponding coefficients for the evaluation of the second group sums were in good agreement with the experimental results with air for the several heat flux distributions. For special heat flux distributions, other kinds of the first group sums may appear in the calculating equation of Nusselt number but it is difficult to evaluate these sums exactly. In these cases the necessary sums can be evaluated approximately with the aid of the already known sums as shown in the case of the exponential heat flux distribution.

In contrast with the prescribed heat flux distribution, the superposed solution for the prescribed wall temperature distribution shows very good convergency. Therefore the corresponding Nusselt number can be accurately calculated with the first three or four eigenvalues and corresponding coefficients at most.

From a study of the fully developed situation it is concluded that the fully developed situation with a generalized temperature profile invariant in the direction of flow is realized by the exponential heat flux distribution alone and the two conditions, the uniform heat flux and the uniform wall temperature, correspond to the special cases of the exponential heat flux distribution.

For special heat flux distribution there exists the quasi-asymptotic situation not so far downstream from the initial heated point. In this situation Nusselt number changes gradually in the axial direction but never reaches the fully developed situation.

Similar method to the proposed approximate one is applicable to the calculation of Nusselt number for arbitrary heat flux distribution in ducts with various cross sections, annular space and space between two parallel plates whose thermal-entry-solutions are obtained as the solutions of the eigen-value problem and take the infinite series expressions.

REFERENCES

1. L. S. Dzung, Heat transfer in a round duct with sinusoidal heat flux distribution, *Proceedings of the Second International Conference on Atomic Energy*, Vol. 7, pp. 657–670 (1958).
2. W. B. Hall and P. H. Price, The effect of a longitudinally varying wall heat flux on the heat transfer coefficient for turbulent flow in a pipe, *Proceedings of the 1961–1962 Heat Transfer Conference*, pp. 607–613. *Am. Inst. Chem. Engrs*, New York (1963).
3. R. Siegel and E. M. Sparrow, Turbulent flow in a circular tube with arbitrary internal heat sources and wall heat transfer, *J. Heat Transfer* **81**, 280–290 (1959).
4. C. A. Sleicher, Jr. and M. Tribus, Heat transfer in a pipe with turbulent flow and arbitrary wall-temperature distribution, *Trans. Am. Soc. Mech. Engrs* **79**, 789–797 (1957).
5. J. R. Sellars, M. Tribus and J. S. Klein, Heat transfer to laminar flow in a round tube or flat conduit the Greatz problem extended, *Trans. Am. Soc. Mech. Engrs* **78**, 441–448 (1956).
6. R. A. Seban and T. T. Shimazaki, Heat transfer to a fluid flowing turbulently in a smooth pipe with wall at constant temperature, *Trans. Am. Soc. Mech. Engrs* 73, 803–809 (1951).
7. R. G. Deissler, Analysis of turbulent heat transfer, mass transfer and friction in smooth tubes at high Prandtl and Schmidt numbers, NACA TN 3145 (1954); also NACA Rep. 1210 (1955).
8. S. Hasegawa and Y. Fujita, Nusselt numbers for fully developed flow in a tube with exponentially varying heat flux, *Mem. Fac. Engng, Kyushu Univ.* **27**, 1–5 (1967).
9. W. M. Kays, *Convective Heat and Mass Transfer*, p. 110. McGraw Hill, New York (1966).
10. Max Jakob, *Heat Transfer*, Vol. 1, p 455. John Wiley, New York (1949).

Résumé—Une méthode approchée est proposée pour prévoir le nombre de Nusselt de l'écoulement turbulent dans un tube avec une distribution de flux de chaleur variant arbitrairement le long de l'axe. L'évaluation de sommes de séries infinies avec une faible convergence est nécessaire pour cette méthode et elle a été effectuée correctement. Les résultats prévus par la méthode proposée ont été vérifiés expérimentalement avec de l'air pour un flux de chaleur uniforme, un flux de chaleur variant exponentiellement et un flux de chaleur variant linéairement. L'appareillage expérimental a été construit de telle façon que le flux de chaleur pourrait se distribuer de la manière imposée en changeant axialement la surface de la section droite de la paroi du tube qui conduit un courant alternatif de faible tension. Les nombres de Nusselt prédits sont en bon accord avec les données expérimentales.

Les conditions pour des distributions de flux de chaleur dans le cas d'un régime entièrement établi avec un profil de température généralisée invariable dans la direction axiale ont été analysées théoriquement. Il en résulte que seul le flux de chaleur variant exponentiellement peut réaliser un régime entièrement établi. Les deux cas du flux de chaleur uniforme et de la température pariétale uniforme, qui réalisent, comme il est bien connu un régime entièrement établi, correspondent à des cas particuliers du flux de chaleur variant exponentiellement.

Zusammenfassung—Es wird eine Näherungsmethode vorgeschlagen zur Bestimmung der Nusselt–Zahl bei turbulenter Rohrströmung mit beliebiger axialer Verteilung der Wärmestromdichte. Hierfür wurde die Berechnung von Summen unendlicher Reihen mit schlechter Konvergenz erforderlich und auch korrekt ausgeführt. Die mit der vorgeschlagenen Methode ermittelten Resultate wurden experimentell nachgeprüft an Luft für gleichförmige, exponentiell und linear veränderliche Wärmestromdichte. Die Versuchsanordnung gestattete es, die Verteilung der Wärmestromdichte in der vorgeschriebenen Weise vorzugeben, indem in axialer Richtung die Querschnittsfläche der von Wechselstrom niedriger Spannung durchflossenen Rohrwandung verändert wurde. Die theoretisch ermittelten Nusselt–Zahlen stimmen gut mit den experimentellen Daten überein.

Die Bedingungen für die Verteilungen der Wärmestromdichte, in voll ausgebildeter Strömung mit unveränderlichen Temperaturprofil in axiale Richtung, wurden theoretisch analysiert. Es ergab sich, dass allein die Wärmestrondichtenverteilung nach der Exponentialfunktion den voll ausgesbildeten Zustand verwirklichen kann. Die beiden Fälle, konstante Wärmestromdichte und konstante Wandtemperatur, die bekanntlich den voll ausgebildeten Zustand verwirklichen, entsprechen den Spezialfällen einer Verteilung der Wärmestromdichte nach der Exponentialfunktion.

Аннотация—Предложен приближенный метод расчета числа Нуссельта для турбулентного течения в трубе с произвольным распределением теплового потока по оси. Для этого метода требуется оценка суммы бесконечного ряда с плохой сходимостью. Полученные с помощью предложенного метода результаты были проверены экспериментально на воздухе с однородным тепловым потоком, с тепловым потоком меняющимся по экспоненте и линейно. Экспериментальная установка сконструирована так, что тепловой поток может распределяться заданным образом вдоль оси за счет изменения площади поперечного сечения стенки трубы, по которой пропускается переменный ток низкого напряжения. Расчетные числа Нуссельта хорошо согласуются с экспериментальными данными.

Теоретически исследованы различные способы распределения теплового потока, которые приводят к развитому течению, когда универсальный профиль температуры не меняется в направлении оси. В результате найдено, что полностью развитое течение возникает только при экспоненциальном распределении теплового потока. Случаи однородного теплового потока и однородной температуры стенки, при которых, как хорошо известно, имеет место полностью развитое течение, относятся к частным случаям экспоненциального теплового потока.